



A model for thickness effect on the band gap of amorphous germanium film

Xiao-Dong Wang, Hai-Feng Wang, Bo Chen, Yun-Peng Li, and Yue-Ying Ma

Citation: [Applied Physics Letters](#) **102**, 202102 (2013); doi: 10.1063/1.4805056

View online: <http://dx.doi.org/10.1063/1.4805056>

View Table of Contents: <http://scitation.aip.org/content/aip/journal/apl/102/20?ver=pdfcov>

Published by the [AIP Publishing](#)



FREE Multiphysics Simulation e-Magazine

DOWNLOAD TODAY >>

 COMSOL

A model for thickness effect on the band gap of amorphous germanium film

Xiao-Dong Wang,^{a)} Hai-Feng Wang, Bo Chen, Yun-Peng Li, and Yue-Ying Ma
 Changchun Institute of Optics, Fine Mechanics and Physics, Chinese Academy of Sciences, Changchun,
 130033, China

(Received 20 November 2012; accepted 23 April 2013; published online 22 May 2013)

A Mott-Davis-Paracrystalline model was proposed to interpret thickness effect of the band gap for amorphous germanium (*a*-Ge). We believe that *a*-Ge has a semiconductor-alloy-like structure, it may contain medium-range order (MRO) and continuous random network (CRN) simultaneously and there is a dependence of MRO/CRN ratio on film thickness and preparation methods/parameters. For MRO is dominant, thickness effect can be described by one-dimensional quantum confinement (ODQC) effect of nanocrystals and strain-induced shrinkage of the band gap; For CRN is dominant, thickness dependence can be interpreted by changes in the quality of a CRN and ODQC effect of nanoamorphous phase. © 2013 AIP Publishing LLC. [<http://dx.doi.org/10.1063/1.4805056>]

Tetrahedral amorphous semiconductors (*a*-Ge, amorphous silicon (*a*-Si)) have attracted much interests among researchers due to their extensive applications in detectors¹ and the semiconductor industry.² Unique optical and electrical properties of *a*-Ge had been interpreted by the continuous random network (CRN) model.³ Radial distribution function (RDF) data deduced from diffraction data provide a seemingly strong evidence that *a*-Ge has only a short-range order (SRO) structure.³ However, RDF analysis is not sensitive to medium-range order (MRO), but fluctuation electron microscopy (FEM)⁴⁻⁷ and variable coherence transmission^{8,9} are able to precisely detect and analyze MRO. Variable coherence transmission data elucidate that MRO indeed exists in *a*-Ge. Strongly strained, topologically crystalline grains are embedded in a largely distorted CRN matrix.⁴⁻⁹

It has been found that there was a decrease in the density,¹⁰ void fraction,^{11,12} and band gap^{12,13} for *a*-Ge films when film thickness increases. It is believed that void fraction, amorphous effect, and one-dimensional quantum confinement (ODQC) effect can be used to interpret thickness dependence of the band gap.^{12,13} However, these interpretations are too simple.

The band gap has a great influence on resistivity of semiconductors. The fact of thickness dependence of the band gap provides a clue that we can control the band gap of *a*-Ge by tuning sample thickness, deposition methods, and volume fraction of MRO. Thus, it is of practical importance to study thickness dependence of the band gap. In addition, Gibson⁵ and Treacy⁴ have published their revolutionary observations that MRO indeed exists in *a*-Ge and *a*-Si. This

profound result provides a clue and base to reconsider intrinsic mechanisms of optical and electrical properties of tetrahedral amorphous semiconductors. In this paper, a Mott-Davis-Paracrystalline (MDP) model combined with ODQC effect is proposed to interpret thickness dependence of the band gap based on Goh's¹³ and Pilione's¹² experiments.

Table I shows Goh's¹³ and Pilione's¹² experimental results and their theoretical interpretation. The value of E_g (0 K) is calculated by Varshni equation¹⁴

$$E_g(T) = E_g(0) - \frac{\alpha T^2}{T + \beta}, \quad (1)$$

where $\alpha = 4.774 \times 10^{-4}$ eV/K and $\beta = 235$ K for *a*-Ge. The band gap ($E_g = 0.66$ eV) of bulk germanium crystals (*c*-Ge) is used for the comparison. Goh's¹³ group prepared *a*-Ge films in the thickness range of 2.6 to 46 nm by the electron beam evaporation (EBE) method. They attributed reduction of the band gap (< 0.66 eV) to amorphous effect, and attributed band gap expansion (> 0.66 eV) to ODQC effect. Amorphous effect was proposed by Goh.¹³ They believed that in amorphous films, the imperfection in the films causes the bands of localized states to broaden, and the band gap may narrow down.¹³ Pilione's¹² group prepared 180–1100 nm *a*-Ge films by the Rf-diode and DC-magnetron sputtering (DC-MS) methods. Rf-diode samples show that the band gap decreases when film thickness increases; while DC-MS samples show a constant value of the band gap when film thickness increases from 180 to 1100 nm. They believed that the band gap decreases resulting from the decrement of the void fraction¹²

$$E_g(A_xB_{1-x}) = \begin{cases} m \leq E_g \leq 0.66, & d > \sim 10 \text{ nm, model-solid theory} \\ 0.66 + C_1/d^2, & d < \sim 10 \text{ nm, ODQC effect of MRO} \\ 0.66 \leq E_g \leq n, & d > \sim 10 \text{ nm, modified Mott-Davis model} \\ 1.05 + C_2/d^2, & d < \sim 10 \text{ nm, ODQC effect of amorphous phase} \end{cases}, \quad x \geq a\% \quad (2)$$

^{a)} Author to whom correspondence should be addressed. Electronic mail: wangxiaodong1978@163.com. Tel.: +086-0431-86176910.

Based on FEM and variable coherence transmission data,⁴⁻⁹ we believe that tetrahedral amorphous semiconductors

TABLE I. Goh's and Pilione's experimental results.

Dominant effect	Thickness d (nm)	E_g (300 K) (eV)	E_g (0 K) (eV)	Deposition method	Reference
Amorphous effect	Bulk	0.66	0.74	EBE	13
	46	0.33	0.41		
	22	0.40	0.48		
ODQC effect	15.3	0.50	0.58	RF-diode sputtering	12
	8.2	0.72	0.80		
	4.7	0.80	0.88		
	2.6	1.03	1.11		
Void fraction	180	0.83	0.91	DC-MS	
	350	0.80	0.88		
	500	0.79	0.87		
	740	0.72	0.80		
	1100	0.74	0.82		
	180–1100	0.83	0.91		

consist of A (topologically crystalline grains (10–20 Å, MRO)) and B (CRN (SRO)). The structure of a -Ge can be defined as A_xB_{1-x} , and x is the volume fraction of MRO. The band gap structure of a -Ge is similar to that of semiconductor alloys.¹⁵ Equation (2) gives a detailed expression of the band-gap structure of a -Ge, and d is film thickness. It must be mentioned that the critical value $a\%$ is only a constant determined by preparation conditions. It has been experimentally found that the volume fraction of MRO can reach approximately 50%.⁵

It is important to note that we believe that the volume fraction of MRO and the quality of a CRN have a great dependence on sample thickness only in some special thickness region for a defined set of deposition conditions.

For x smaller than the critical value $a\%$, and B (CRN) is dominant, then the band gap exhibits distinct characters of amorphous phase, which can be interpreted by modified Mott-Davis model¹⁶ and ODQC effect of amorphous phase. As shown in Eq. (2), for $d > \sim 10$ nm, the band gap narrows down due to a decrease in quality of the CRN structure with the increment of thickness; for $d < \sim 10$ nm, band gap broadens as compared to bulk a -Ge due to ODQC effect of amorphous phase.

Quantum confinement effect is derived from Heisenberg uncertainty principle. According to Heisenberg uncertainty principle, we know that if a particle is confined to a region of the x axis of length Δx , then an uncertainty in its momentum is obtained by $\Delta p_x \sim \hbar/\Delta x$. The confinement in x direction results in an additional kinetic energy $\Delta E = E_{\text{confinement}} = (\Delta p_x)^2/2m \sim \hbar^2/(2m(\Delta x)^2)$.¹⁷ In this paper, the confinement is only in film thickness d direction, so it is ODQC. More details about ODQC can be found in Refs. 13 and 17. Thickness dependence of the band gap due to ODQC is described by

$$E_g(d) = E_{\text{bulk}} + C/d^2, \quad (3)$$

where C is defined as¹⁸

$$C = \frac{\pi^2 \hbar^2}{2} \left(\frac{1}{m_e^*} + \frac{1}{m_h^*} \right), \quad (4)$$

where m_e^* and m_h^* are the electron and hole effective mass, respectively. The value of E_{bulk} is determined by the structure of ultrathin films. If the CRN is dominant, E_{bulk} is 1.05 eV; If MRO is dominant, E_{bulk} is 0.66 eV.¹⁹ Equation (5)¹⁹ demonstrates the details about thickness dependence

due to ODQC effect for germanium nanocrystals (nc -Ge) and nanoamorphous germanium (na -Ge), respectively

$$\{ E_g(d) = 0.66 + 16.8/d^2 \quad nc - Ge, \quad (5.1)$$

$$\{ E_g(d) = 1.05 + 10.3/d^2 \quad na - Ge, \quad (5.2)$$

Figure 1(a) demonstrates the structure of modified Mott-Davis model, which is cited from Figure 9 of Ref. 20 and Figure 8 of Ref. 21. As shown in Figure 1(a), the shaded area represents the region of localized states, E_0 is the interval between the localized states tail of the conduction band and the localized states tail of the valence band, E_{g1} (E_{g2}) is the interval between extended states of the conduction (valence) band and the localized states tail of the valence (conduction) band, and E_g is the interval between extended states of the conduction and valence band, which is the mobility gap. Optical band gap is equal to E_{g1} (E_{g2}).^{16,20,21} E_{g1} is assumed to have a same value with E_{g2} . Transitions between localized states are ignored due to their insignificance.^{16,20,21} We believe that the band gap narrows down with the increment of film thickness in some special thickness region. It was reported that E_0 of high-quality CRN is 1.3 eV (0 K).²² Thus, the band gap can broaden to be larger than 1.3 eV. The band gap varies between 0.66 and n (>1.3) eV due to different quality of the CRN (as shown in Eq. (2)). The CRN is not a unique structure, and CRN structures have different band gaps due to diverse strains and defects. The reduction of the band gap is relying on the quality of the CRN. The effects of quantitative disorder on the band gap have been elaborately discussed by Tanaka²³ group. The main differences between our arguments and Mott-Davis model include: (1) the mobility gap is not fixed, it can be changed due to the extent of disorder and the quality of a CRN; (2) optical band gap is not some special fixed value, it can decrease due to worsening of the CRN quality as the thickness increases in a special thickness region.

$$(\Delta\rho/\rho)_{\text{pure}} = \Delta E_g/2kT. \quad (6)$$

In addition, we can also analyze electrical conduction mechanism of a -Ge. At room temperature, electrons in localized states of the valence band (LVB) can transfer to extended states of the conduction band (ECB) by thermal

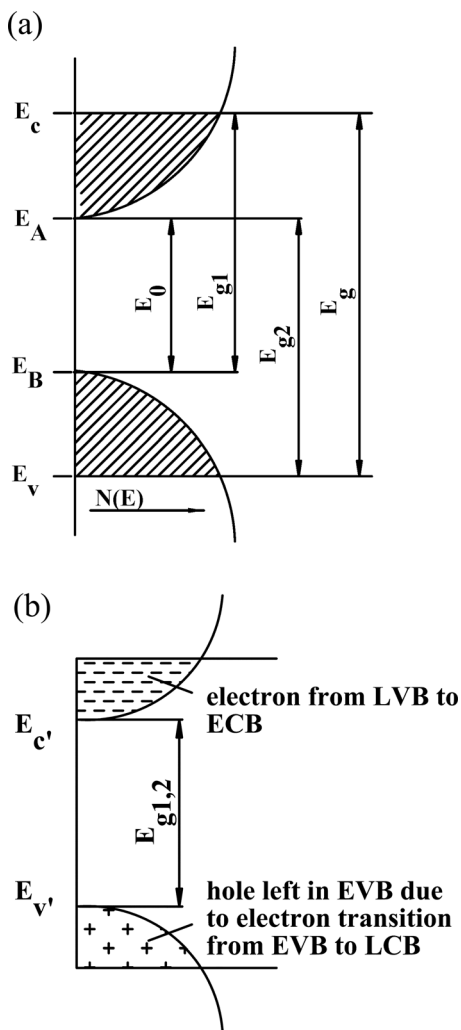


FIG. 1. (a) Mott-Davis model (see Refs. 20 and 21) of the density of states function for *a*-Ge films, and (b) conduction mechanism of *a*-Ge at room temperature. Reprinted with permission from S. G. Tomlin, E. Khawaja, and G. K. M. Thutupalli, J. Phys. C 9, 4335 (1976). Copyright 1976 IOP Publishing. Reprinted with permission from G. K. M. Thutupalli and S. G. Tomlin, J. Phys. C 10, 467 (1977). Copyright 1977 IOP Publishing.

activation, and electrons in extended states of the valence band (EVB) can transfer to localized states of the conduction band (LCB) by thermal activation. As shown in Figure 1(b), electrons in ECB and holes in EVB contribute most to the conduction of *a*-Ge films. The contribution of holes in LVB and electrons in LCB to the electrical conduction is ignored due to their very low mobilities.¹⁶ Thus, a dependence of the change in band gap on the change in resistivity can be qualitatively described by Eq. (6).²⁴ This equation is very simple because the number of electrons in ECB and holes in EVB is assumed to be same for an intrinsic semiconductor.²⁴ As a proof, Pandya²⁵ described that film resistivity decreases as the thickness increases.

For x larger than the critical value $a\%$, and A (MRO) is dominant, then the band gap shows significant features of MRO, which can be interpreted by the model-solid theory²⁶ and ODQC effect of MRO. As shown in Eq. (2), for $d > \sim 10$ nm, the band gap narrows down as the strain is exerted on high volume fraction of topologically crystalline grains; for $d < \sim 10$ nm, the band gap broadens as compared to *c*-Ge due to ODQC effect of MRO (Eq. (5.1)). The strain

causes the topologically crystalline grains deformed and distorted, which can narrow down the band gap.^{6,7} However, the band gap cannot decrease to be zero, and it should be larger than a constant value of m . So far, we still cannot give a specific value for the parameter m . The band gap varies between m and 0.66 eV resulting from different volume fraction of MRO. The higher the volume fraction of MRO is, the larger the strain is, and the smaller the band gap is. The reduction of the band gap is dependent on the strain exerted on topologically crystalline grains.²⁷⁻²⁹

Thus, a MDP model combined with ODQC effect is proposed to describe the band gap of *a*-Ge films with A_xB_{1-x} structure.

We have given Goh's and Pilione's experimental results and their discussions, now we can use our MDP model to discuss all these experimental results.

First, we interpret Goh's experimental results. In their experiment, *a*-Ge films were prepared by the EBE technique. We assume that MRO is dominant in their samples because MRO was discovered in *a*-Ge films deposited by the EBE technique.

For $d < \sim 10$ nm, due to ODQC effect of MRO, the band gap expands to be 0.80 eV (4.7 nm) and 1.03 eV (2.6 nm).¹³ The plot of $E_g(d) \sim d^{-2}$ at 300 K is shown in Figure 2(a). The slope of the least-square-fitting line is 2.31, and the intercept at y-axis is 0.69 eV, which is 0.03 eV smaller than 0.66 eV, which is in good agreement with Eqs. (2) and (5.1). The fitting formula is described by

$$E_g(d) = 0.69 + 2.31/d^2. \quad (7)$$

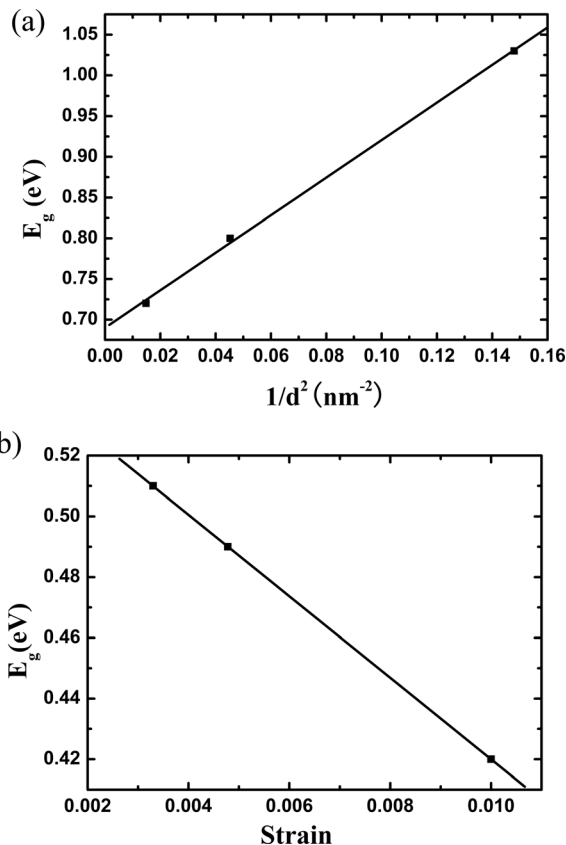


FIG. 2. Goh's experimental results: (a) d^{-2} dependence on E_g (300 K; 2.6, 4.7, and 8.2 nm), and (b) strain dependence on the band gap (0 K; 15.3, 22, and 46 nm).

The main difference between Eqs. (5.1) and (7) is the value of C_1 , and 2.31 is much smaller than 16.8. This significant deviation may be due to the existent of less CRN and strain

$$\Delta E_g = a_v \Delta \Omega / \Omega, \quad (8)$$

$$a_v = a_{c,av} - a_{v,av}, \quad (9)$$

$$E_v = E_{v,av} + \Delta_0 / 3, \quad (10)$$

$$\Delta \Omega / \Omega = \text{Tr}(\varepsilon) = (\varepsilon_{xx} + \varepsilon_{yy} + \varepsilon_{zz}). \quad (11)$$

For $d > \sim 10$ nm, due to strain-induced shrinkage, the band gap narrows down to be 0.4 eV (22 nm) and 0.33 eV (46 nm).¹³ We assume that the band gap is linearly changed with the strain exerted on topologically crystalline grains, and the strain is linearly dependent on film thickness. The variation in band gap with the change in strain can be described by Eqs. (8)–(11) of the model-solid theory.²⁶ $\Delta \Omega / \Omega$ is the fractional volume change, which determines hydrostatic contribution of the strain; a_v is the band-gap deformation potential, and $a_{v,av}$ and $a_{c,av}$ are the hydrostatic deformation potentials for the valence band and conduction band, respectively; Δ_0 is spin-orbit splitting, which is 0.30 eV for Ge.²⁶ The strain exerted on topologically crystalline grains of the 46 nm film is assumed to be 1%.³⁰ Figure 2(b) demonstrates strain dependence on the band gap (0 K; 15.3, 22, and 46 nm). The intercept at y-axis is 0.55 eV, which is 0.19 eV smaller than 0.74 eV (indirect band gap of *c*-Ge, $\Gamma_v \rightarrow L_c$), and 0.37 eV smaller than 0.92 eV (direct band gap of *c*-Ge, $\Gamma_v \rightarrow \Gamma_c$).³¹ The slope of least-square-fitting line is -13.42 , which is in good agreement with $a_{v, \text{direct}}$ of references, -12.7 ,²⁷ -11.2 ,²⁸ and -11.5 .²⁹

It was found by Tomlin²⁰ that the band gap increases due to a narrowing of the bands of localized states from 0.30 to 0.18 eV after 300 °C annealing. Moreover, it is known that post-annealing can make MRO transform into the CRN. Correspondingly, the band gap should broaden when the strain exerted on grains decreases or the CRN is dominant due to a transformation from MRO to a CRN. However, there is still no experimental data to support this prediction. Thus, it is much more complicated to analyze the band gap of *a*-Ge after thermal annealing.

As for Pilione's experimental results, their samples were prepared by the sputtering method. It is still in debate that whether MRO exists in *a*-Ge films prepared by MS method.^{8,9} Here, we assume that the CRN is dominant in Pilione's samples. For DC-MS sample, the volume fraction of the CRN is fixed and the structure is stable in this thickness region, so they show no variations of the band gap when sample thickness increases.¹² Only Rf-diode samples show thickness dependence of the band gap. In the thickness range of 180 to 740 nm, we assume that the band gap is linearly changed with film thickness. The thicker the sample is, the worse the CRN quality is, and the less the band gap is. The width of localized states is assumed to be 0.3 eV.²⁰ E_0 can be obtained by $E_{g1,2} - 0.3$ eV. Figure 3 shows thickness dependence of E_0 (0 K; 180, 350, 500, and 740 nm) in Pilione's experimental results, and the intercept of least-square-fitting line at y-axis is 0.65 eV, which is 0.65 eV

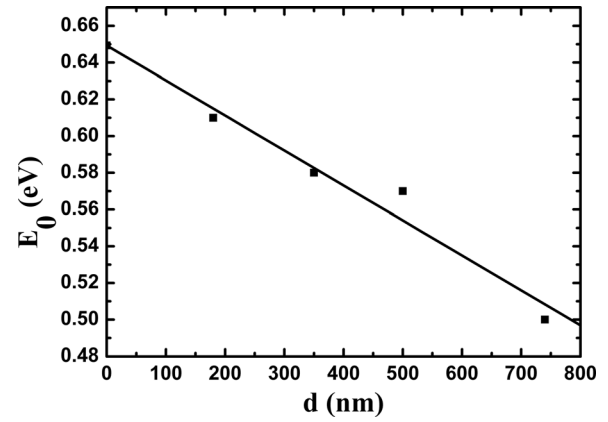


FIG. 3. Pilione's experimental results: thickness dependence on E_0 (0 K; 180, 350, 500, and 740 nm).

smaller than 1.3 eV. This may be because that ideal high-quality CRN is hardly achieved in this deposition process. Substrate heating and post-annealing are needed to make *a*-Ge close to ideal high-quality CRN.^{16,20,21} In addition, above 740 nm, there are more factors that influence the band gap of *a*-Ge, so no such thickness effect occurs.

However, for thickness smaller than ~ 10 nm, there is a lack of experimental data about *a*-Ge prepared by the MS technique. Thus, we cannot verify the validity of Eq. (5.2) for describing thickness effect due to ODQC effect of amorphous phase when the CRN is dominant in *a*-Ge. This still needs further investigations.

Treacy and Gibson^{8,9} pointed out that the deposition rate, substrate heating, and vacuum deposition are three key factors that contribute most to the formation of MRO in *a*-Ge or *a*-Si films. Until now, only *a*-Ge films deposited by the thermal evaporation method are proved to have a paracrystalline structure, and studies of MS-deposited samples have not yet led to a clear conclusion because they involve vacuum depositions with simultaneous ion bombardment.^{8,9} The details about a dependence of MRO on preparation methods are shown in Refs. 8 and 9.

It was reported that MRO is inclined to be formed in *a*-Ge films prepared by the EBE technique. The CRN is thermally stable state of amorphous tetrahedral semiconductors due to its lowest energy, and topologically crystalline grains are prone to be formed for symmetry reasons during the deposition process. There is a competition between the trend of retaining topologically crystalline grains and approaching to the lowest energy during the film preparation.^{5,8,9} We predict that the augment of atoms and the activation energy from substrate heating contribute to the formation of Schläfli clusters.³² This may be the reason for thickness dependence of MRO for *a*-Ge film ($d > \sim 10$ nm) prepared by the EBE method.

It seems that the CRN is prone to be formed in *a*-Ge films deposited by the MS method. Within a special thickness range, with the increasing number of atoms, more defects appear, and the CRN quality gets worse. This may be the reason for thickness dependence of the CRN quality for *a*-Ge film ($d > \sim 10$ nm) deposited by the MS method.

In summary, a MDP model combined with ODQC effect is proposed to interpret thickness dependence of the band gap for *a*-Ge. We believe that *a*-Ge has a $A_x B_{1-x}$ structure, it

may contain MRO and SRO simultaneously and there is a dependence of MRO/SRO ratio on film thickness and preparation methods/parameters. When MRO is dominant, thickness effect of band gap shows significant feature of MRO, and it can be described by ODQC effect of MRO and model-solid theory; When the CRN is dominant, thickness effect of band gap shows significant feature of amorphous phase, and it can be interpreted by ODQC effect of amorphous phase and modified Mott-Davis model. Moreover, electrons in ECB and holes in EVB contribute most to the conduction of *a*-Ge films.

In addition, some workers³³ argued that the volume fraction of MRO is small, while Gibson^{5–7} group believed that it is approximately 50%. This controversy is probably resulting from their different sample thickness and deposition methods. Therefore, our findings can also shed some light on remained controversy about the volume fraction of MRO. More importantly, there is a great promise in developing a technique to tune the band gap or shift from indirect band to direct band simply by adjusting film thickness and preparation parameters instead of externally applied strain.

This work was supported by the National Natural Science Foundation of China (Grant No. 10878004).

¹O. Jagutzki, J. S. Lapington, V. Mergel, H. Schmidt-Böcking, U. Spillmann, and L. B. C. Worth, *Nucl. Instrum. Methods Phys. Res. A* **477**, 256–261 (2002).

²W. Shockley, *Bell Syst. Tech. J.* **28**, 435 (1949).

³R. J. Temkin, W. Paul, and G. A. N. Connell, *Adv. Phys.* **22**, 581 (1973).

⁴M. M. J. Treacy and K. B. Borisenko, *Science* **335**, 950 (2012).

⁵J. M. Gibson, *Science* **335**, 929 (2012).

⁶J. M. Gibson, M. M. J. Treacy, T. Sun, and N. J. Zaluzec, *Phys. Rev. Lett.* **105**, 125504 (2010).

⁷P. M. Voyles, Z. Zotov, S. M. Nakhmanson, D. A. Drabold, J. M. Gibson, M. M. J. Treacy, and P. Keblinski, *J. Appl. Phys.* **90**, 4437 (2001).

⁸J. M. Gibson and M. M. J. Treacy, *Phys. Rev. Lett.* **78**, 1074 (1997).

⁹M. M. J. Treacy, J. M. Gibson, and P. J. Keblinski, *J. Non-Cryst. Solids* **231**, 99 (1998).

¹⁰J. R. Blanco, P. J. McMarr, J. E. Yehoda, K. Vedam, and R. Messier, *J. Vac. Sci. Technol. A* **4**, 577 (1986).

¹¹P. J. McMarr, J. R. Blanco, K. Vedam, R. Messier, and L. Pilione, *Appl. Phys. Lett.* **49**, 328 (1986).

¹²L. J. Pilione, K. Vedam, J. E. Yehoda, R. Messier, and P. J. McMarr, *Phys. Rev. B* **35**, 9368 (1987).

¹³E. S. M. Goh, T. P. Chen, C. Q. Sun, and Y. C. Liu, *J. Appl. Phys.* **107**, 024305 (2010).

¹⁴Y. P. Varshni, *Physica (Utrecht)* **34**, 149 (1967).

¹⁵M. Jaros, *Rep. Prog. Phys.* **48**, 1091–1154 (1985).

¹⁶N. F. Mott, *Conduction in Non-crystalline Materials* (Clarendon Press, Oxford, 1993), p. 86.

¹⁷M. Fox, *Optical Properties of Solids* (Oxford University Press, Oxford, 2001), p. 115.

¹⁸P. J. van den Oever, M. C. M. van de Sanden, and W. M. M. Kessels, *J. Appl. Phys.* **101**, 123529 (2007).

¹⁹O. Dag, E. J. Henderson, and G. A. Ozin, *Small* **8**(6), 921–929 (2012).

²⁰S. G. Tomlin, E. Khawaja, and G. K. M. Thutupalli, *J. Phys. C* **9**, 4335 (1976).

²¹G. K. M. Thutupalli and S. G. Tomlin, *J. Phys. C* **10**, 467 (1977).

²²G. T. Barkema and N. Mousseau, *Phys. Rev. B* **62**, 4985–4990 (2000).

²³K. Tanaka and R. Tsu, *Phys. Rev. B* **24**, 2038 (1981).

²⁴J. H. Taylor, *Phys. Rev.* **80**, 919–920 (1950).

²⁵D. K. Pandya, A. C. Rastogi, and K. L. Chopra, *J. Appl. Phys.* **46**, 2966 (1975).

²⁶C. G. Van de Walle, *Phys. Rev. B* **39**, 1871 (1989).

²⁷A. Blacha, H. Presting, and M. Cardona, *Phys. Status Solidi B* **126**, 11 (1984).

²⁸F. Zhang, V. H. Crespi, and P. Zhang, *Phys. Rev. Lett.* **102**, 156401 (2009).

²⁹B. Weber and M. Cardona, *Phys. Rev. B* **15**, 875 (1977).

³⁰M. M. J. Treacy, private communication (2012).

³¹H. Tahini, A. Chroneos, R. W. Grimes, U. Schwingenschlögl, and A. Dimoulas, *J. Phys.: Condens. Matter* **24**, 195802 (2012).

³²M. M. J. Treacy, P. M. Voyles, and J. M. Gibson, *J. Non-Cryst. Solids* **266–269**, 150–155 (2000).

³³S. N. Bogle, P. M. Voyles, S. V. Khare, and J. R. Abelson, *J. Phys. Condens. Matter* **19**, 455204 (2007).